ChemPubSoc Europe

DOI: 10.1002/cmdc.201500447

CHEMMEDCHEM Full Papers

Design, Synthesis and Evaluation of Triazole-Pyrimidine Analogues as SecA Inhibitors

Jianmei Cui,[a] Jinshan Jin,[b] Arpana Sagwal Chaudhary,[a] Ying-hsin Hsieh,[b] Hao Zhang,[b] Chaofeng Dai,[a] Krishna Damera,[a] Weixuan Chen,[a] Phang C. Tai,*[b] and Binghe Wang*[a]

SecA, a key component of the bacterial Sec-dependent secretion pathway, is an attractive target for the development of new antimicrobial agents. Through a combination of virtual screening and experimental exploration of the surrounding chemical space, we identified a hit bistriazole SecA inhibitor, SCA-21, and studied a series of analogues by systematic dissections of the core scaffold. Evaluation of these analogues allowed us to establish an initial structure–activity relationship in SecA inhibition. The best compounds in this group are potent inhibitors of SecA-dependent protein-conducting channel activity and protein translocation activity at low- to sub-micromolar concentrations. They also have minimal inhibitory concentration (MIC) values against various strains of bacteria that correlate well with the SecA and protein translocation inhibition data. These compounds are effective against methicillin-resistant *Staphylococcus aureus* strains with various levels of efflux pump activity, indicating the capacity of SecA inhibitors to null the effect of multidrug resistance. Results from studies of drug-affinity-responsive target stability and protein pull-down assays are consistent with SecA as a target for these compounds.

Introduction

Because of drug resistance issues, bacterial pathogens have re-emerged as a serious public health concern.[1] There is an urgent need to develop new antimicrobials, especially those with novel mechanisms of action. Common antibiotic mechanisms include inhibition of essential processes in the bacterium to disrupt replication, transcription, translation, or cell-wall synthesis.[2] Recently, SecA, a key enzyme in protein translocation,[3] has drawn interest in the development of antimicrobial agents[4] because of its unique role in bacterial survival, virulence factor secretion, and membrane integration of certain efflux pumps, which are responsible for multidrug resistance.[5]

In both Gram-positive and Gram-negative bacteria, the majority of secretory proteins, including virulence factors, are translocated across the cytoplasmic membrane through the Sec-dependent pathway. SecA is the central component of the Sec-dependent secretion pathway,[3e,6] interacting with virtually all the other components of the system, acting as a molecular chaperone and motor, and providing the driving force for protein translocation.[7] In addition, SecA has been shown to form a protein-conducting channel in the presence of phospholipid bilayers.[8] SecA is required for bacterial viability and virulence, and is highly conserved in bacteria with no human counterpart.[9] Targeting SecA therefore represents a unique strategy to combat bacterial pathogens with minimal human toxicity. In our previous studies, pyrimidine analogues were developed from virtual screening against an *Escherichia coli* (*Ec*)SecA crystal structure.[10] By screening related compounds, we identified one bistriazole compound (**1**, SCA-21, Figure 1), which inhibits both the intrinsic ATPase activity and translocation ATPase activity of *Ec*SecA, with an IC_{50} value of ~30 μM. By dissecting this hit, we designed and synthesized roughly 40 analogues, among which some (such as **7b** and **12a**) were found to potently inhibit SecA-dependent activities at high-nanomolar to low-micromolar concentrations in an in vitro (vesicle) protein translocation study and an ion channel oocyte assay. The inhibition of these functional activities correlates with the inhibition of bacterial growth.

Results and Discussion

Chemistry

SCA-21 has a pyrimidine core conjugated to two substituted triazoles in a symmetric fashion by a thioether bond. Notably, these triazoles are 1,2,4-triazoles, which are different from the 1,2,3-triazoles synthesized via [2+3] cycloaddition reaction between an organic azido compound and an alkyne. To improve its potency and understand its structure–activity relationships (SAR), we started to simplify the structure by dissecting the hit compound in half and removing part **A**. Figure 1 shows the

[a] J. Cui,[+] A. S. Chaudhary, C. Dai, K. Damera, W. Chen, B. Wang
Department of Chemistry
Georgia State University, Atlanta, GA 30303 (USA)
E-mail: wang@gsu.edu

[b] J. Jin,[+] Y.-h. Hsieh, H. Zhang, P. C. Tai
Department of Biology, Center for Biotechnology and Drug Design and Center for Diagnostics and Therapeutics
Georgia State University, Atlanta, GA 30303 (USA)
E-mail: biopct@gsu.edu

[+] These authors contributed equally to this work.

Supporting information for this article is available on the WWW under http://dx.doi.org/10.1002/cmdc.201500447.

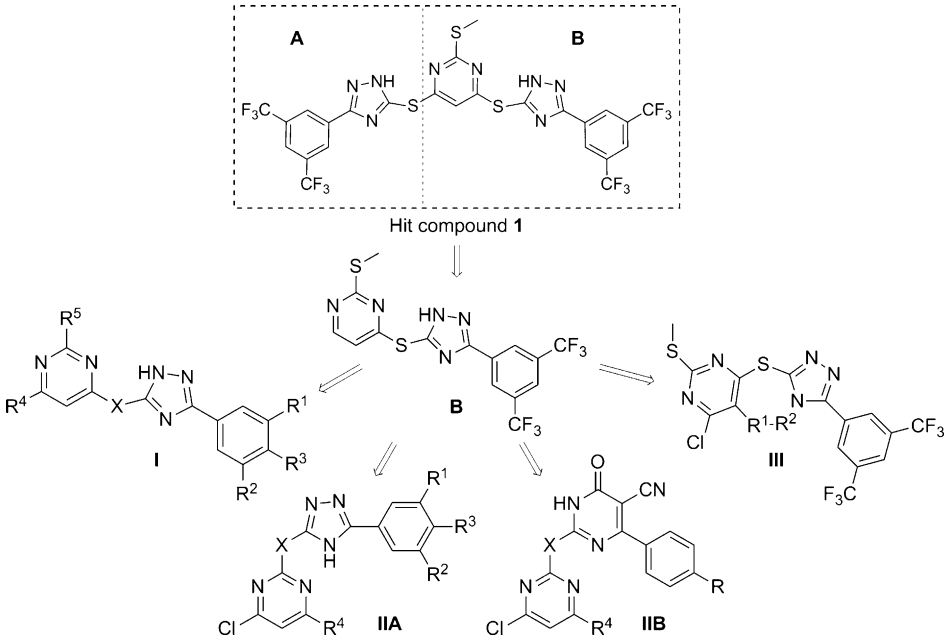

Figure 1. Optimization of the hit compound SCA-21.

general strategy of analogue design. Specifically, the plan was to examine substitution effects in scaffold **I**, positional effects in scaffold **IIA**, the importance of the triazole ring in scaffold **IIB**, and the effect of conformational constraints around the triazole and pyrimidine axis in scaffold **III**.

We were interested in modifying scaffold **I** by changing six different groups (R^1–R^5 and X; Figure 1). Synthesis started by reacting commercially available benzoyl chloride **2** with hydrazine carboamide **3**, followed by self-condensation of **4** in the presence of 5% sodium hydroxide under reflux conditions to yield **5** (Scheme 1).[11]

The triazole-pyrimidine analogues **7**, **9**, **12**, and **15** were then synthesized by reacting key intermediate **5** under weakly basic conditions with the appropriately substituted pyrimidines (Schemes 2 and 3). Series **7** has a methylthio ether group at the 2-position, whereas series **9** does not. In series **12**, the methylthio ether was replaced by either a bulkier thioether or an oxoether.

Scheme 3 describes the synthesis of compound **15**, which contains scaffold **I**, but with an oxadiazole instead of a triazole linking the pyrimidine and phenyl rings. Compound **15** was synthesized by first reacting commercially available 3,5-bis(trifluoromethyl)benzhydrazide (**13**) with carbon disulfide to give **14**.[12] Subsequent reaction of **14** with 4,6-dichloro-2-(methylthio)pyrimidine (**6b**), under weakly basic conditions, gave compound **15**.[13]

Analogues with scaffold **II** (Figure 1) were designed to evaluate the effect of regioisomerism, that is, whether the given substitution is at positions 2 or 4 of the pyrimidine ring (compounds **16**–**18**) as well as the importance of the triazole ring (compound **20**). Scheme 4 illustrates the synthesis of compounds **16**–**18** and **20**. Specifically, they were synthesized by reaction of intermediates **5**, **14**, or **19** with 2,4,6-trichloro pyrimidine compounds under weakly basic conditions at room temperature.[12]

Analogues of scaffold class **III** (Figure 1) were designed to examine the importance of conformational constraints, espe-

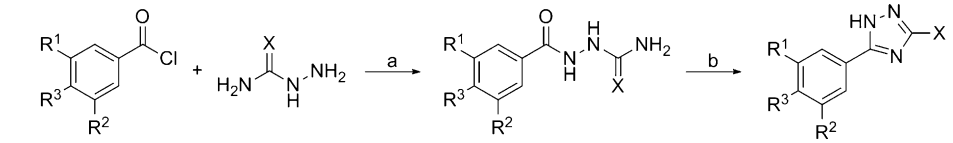

2a: R^1=R^2=CF_3, R^3=H
2b: R^1=F, R^2=H, R^3=H
2c: R^1=R^2=F, R^3=H
2d: R^1=R^2=H, R^3=CF_3
2e: R^1=R^2=OCH_3, R^3=H
2f: R^1=R^2=CH_3, R^3=H

3a: X=S
3b: X=NH
3c: X=O

4a: R^1=R^2=CF_3, R^3=H, X=S
4b: R^1=R^2=CF_3, R^3=H, X=NH
4c: R^1=R^2=CF_3, R^3=H, X=O
4d: R^1=F, R^2=H, R^3=H, X=S
4e: R^1=R^2=F, R^3=H, X=S
4f: R^1=R_2=OCH_3, R^3=H, X=S
4g: R^1=R^2=H, R^3=CF_3, X=S
4h: R^1=R^2=CH_3, R^3=H, X=S

5a: R^1=R^2=CF_3, R^3=H, X=SH
5b: R^1=R^2=CF_3, R^3=H, X=NH_2
5c: R^1=R^2=CF_3, R^3=H, X=OH
5d: R^1=F, R^2=H, R^3=H, X=SH
5e: R^1=R^2=F, R^3=H, X=SH
5f: R^1=R^2=OCH_3, R^3=H, X=SH
5g: R^1=R^2=H, R^3=CF_3, X=SH
5h: R^1=R^2=CH_3, R^3=H, X=SH

Scheme 1. *Reagents and conditions*: a) THF, 0 °C→RT, overnight; b) 5% NaOH, reflux, 5 h, 65–87% overall yields.

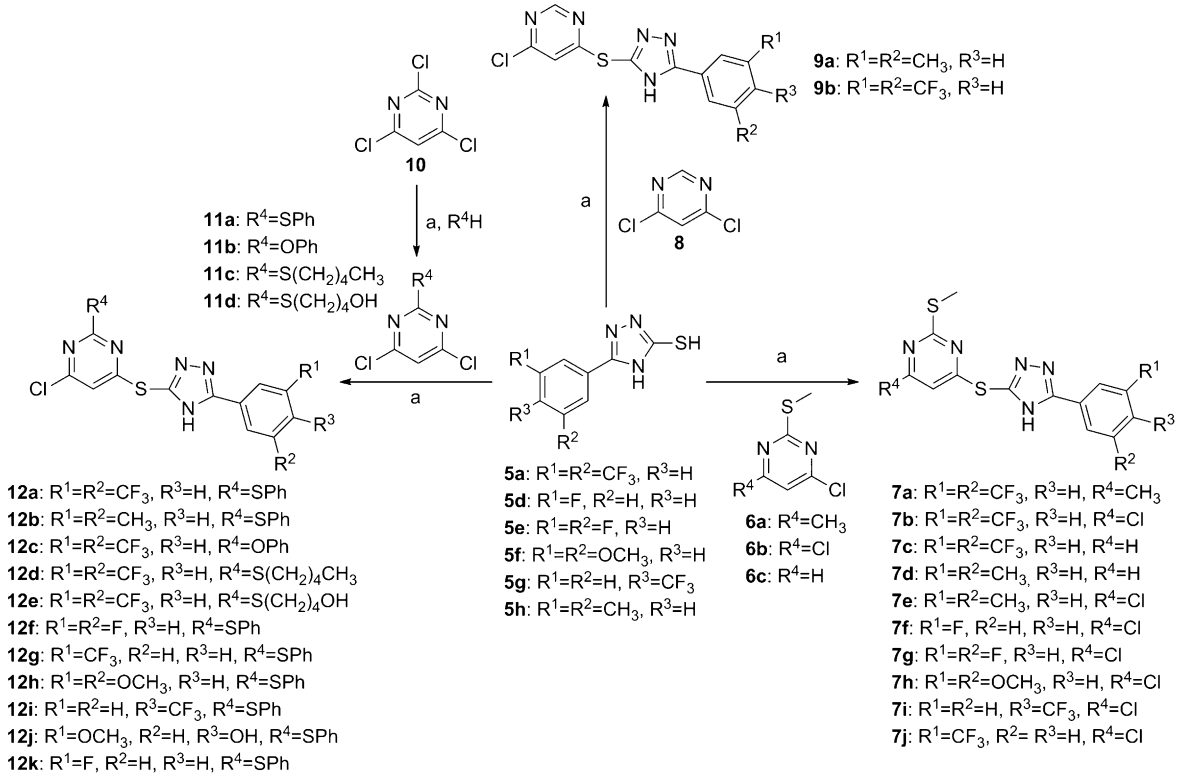

Scheme 2. *Reagents and conditions*: a) K_2CO_3, acetone, RT, 2–3 h, 35–80 %.

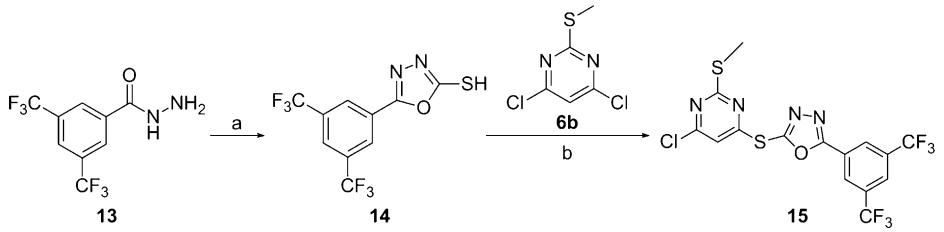

Scheme 3. *Reagents and conditions*: a) CS_2, H_2O/EtOH, reflux, 5 h, 65 %; b) K_2CO_3, acetone, RT, 2–3 h, 80 %.

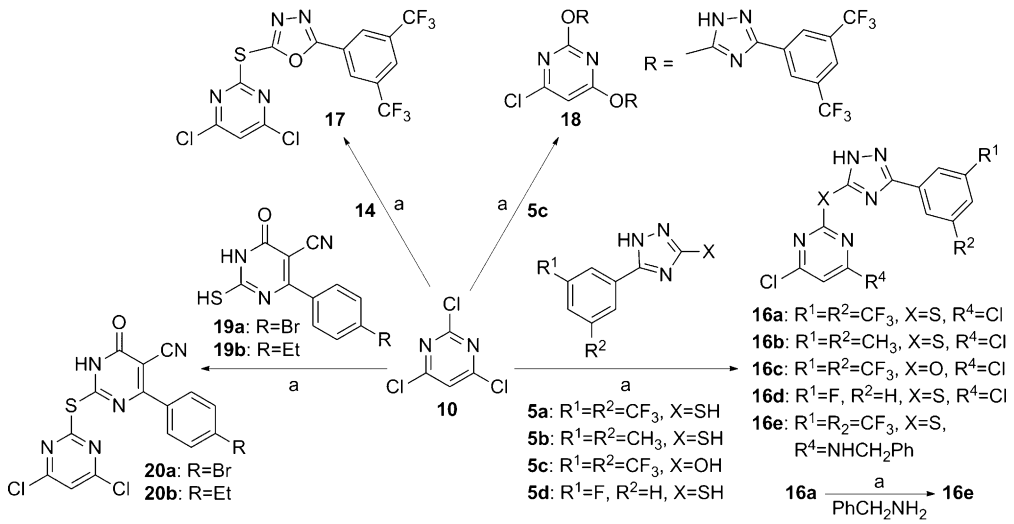

Scheme 4. *Reagents and conditions*: a) K_2CO_3, acetone, RT, 2–3 h, 35–80 %.

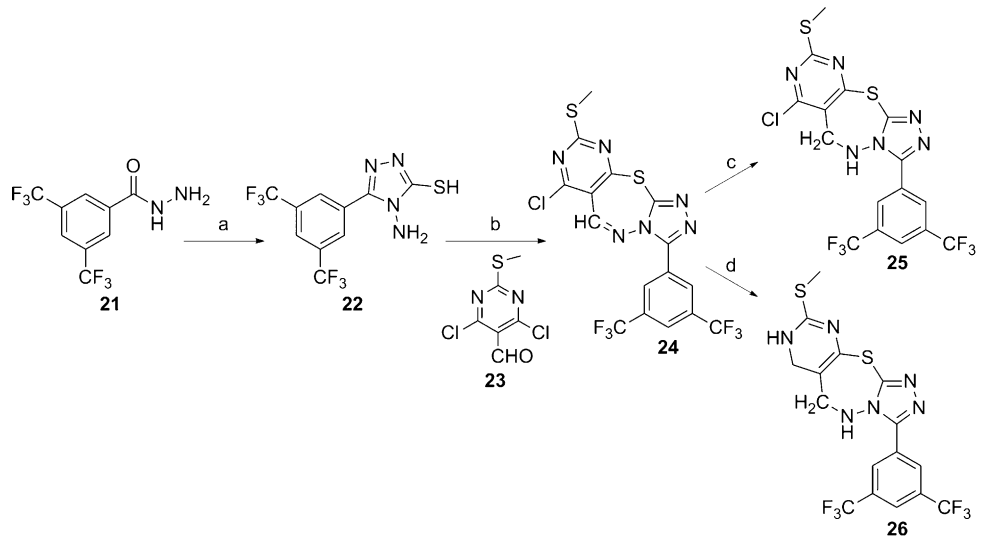

Scheme 5. *Reagents and conditions*: a) CS_2, NH_2NH_2, KOH/EtOH, 82%; b) DMF, 60 °C, 4 h, 76%; c) $NaBH_4$ (1 equiv), EtOH, RT, 2 h, 82%; d) $NaBH_4$ (10 equiv), EtOH, RT, 2 h, 40%.

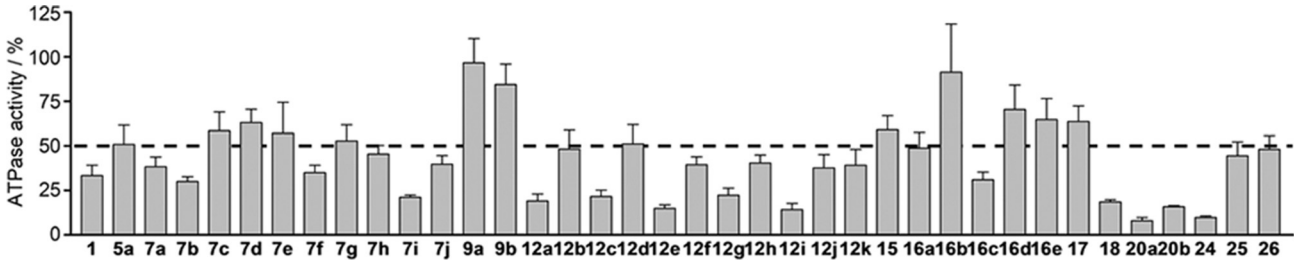

Figure 2. Screening for inhibition of the ATPase activity of *Ec*SecAN68: The initial screening assays were carried out at 50 μM for all compounds.

cially around the triazole and pyrimidine axis. Compound **22** was synthesized from commercially available 3,5-bis(trifluoromethyl)benzhydrazide **21** by reaction with carbon disulfide under strongly basic conditions (Scheme 5).[12] Then reaction of **22** with 4,6-dichloro-2-(methylthio)pyrimidine-5-carbaldehyde (**23**) gave compound **24**. Compounds **25** and **26** were synthesized by reduction of **24** with varying equivalents of sodium borohydride at room temperature.[14]

Biological evaluation

We first evaluated the inhibitory effect against the intrinsic ATPase activity of *Ec*SecAN68, which is a truncated form of *E. coli* SecA that lacks the inhibitory/regulatory C terminus.[10b,15] In previous publications, we discussed in detail the advantages and disadvantages of various assays in screening for SecA inhibitory activities, and the need to use more than one assay for validations.[4c,16] Briefly, we recognize that this is not an ideal assay because *Ec*SecAN68 may very well have a different conformation from that of the membrane-bound form in live bacteria, and the *E. coli* form may not represent the SecA from both Gram-positive and Gram-negative species. However, this assay allows rapid screening of a large number of compounds, and all the other assays are of low throughput.[10b,15] We also used antimicrobial assays as a gatekeeper to ensure that we examine all compounds with potent antimicrobial activities, regardless of the results from the *Ec*SecAN68 assay. We used two representative strains for antimicrobial assays: a Gram-positive strain (*S. aureus* 6538) and a Gram-negative strain (*E. coli* NR698),[4c,10b,17] the latter of which has an outer-membrane mutation resulting in increased drug permeability. Initial screening was conducted at a test compound concentration of 50 μM (Figure 2). There were 22 compounds that showed greater than 50% inhibition at this concentration. These compounds were then evaluated further at various concentrations to allow the determination of IC_{50} values (Tables 1–3). Two class **I** compounds, **7b** and **12a**, showed significant enzyme inhibitory activities at low-micromolar concentrations. Notably, the analogue with the pyrimidine ring removed, **5a**, showed lower activity. Such results suggest that both the triazole and pyrimidine rings are very important for inhibitory activity. Changing the position of the triazole ring substituent to the 2-position (class **II**, Figure 1, Table 2) decreases the inhibitory activity; conformationally constrained analogues (class **III**, Figure 1, Table 3) also did not yield active compounds.

For class **I** compounds, adding a chloro group as the R^4 substituent significantly increased inhibitory effect (**7b**, Table 1). Replacing one or both trifluoromethyl R^1 and R^2 groups with

Table 1. SAR studies for class I compounds.

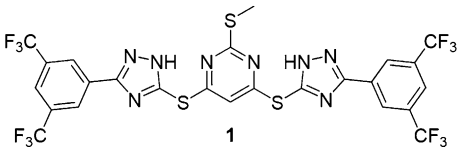

1

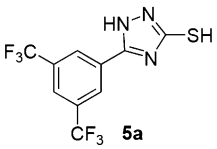

5a

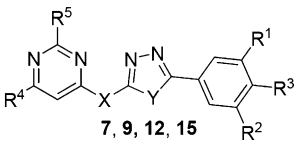

7, 9, 12, 15

Compd	SCA	R^1	R^2	R^3	X	R^4	R^5	Y	IC_{50} [μM][a] *Ec*SecAN68	MIC [μM][b] *E. coli* NR698	MIC [μM][b] *S. aureus* 6538
1	SCA-21	N/A	N/A	N/A	N/A	N/A	N/A	N/A	25.0	25.0	12.5
5a	SCA-126	$-CF_3$	$-CF_3$	-H	-SH	N/A	N/A	-NH-	60.0	>250.0	>250.0
7a	SCA-128	$-CF_3$	$-CF_3$	-H	-S-	$-CH_3$	$-SCH_3$	-NH-	25.0	33.3	18.8
7b	SCA-107	$-CF_3$	$-CF_3$	-H	-S-	-Cl	$-SCH_3$	-NH-	30.0	4.7	3.1
7c	SCA-123	$-CF_3$	$-CF_3$	-H	-S-	-H	$-SCH_3$	-NH-	95.0	50.0	62.5
7d	SCA-117	$-CH_3$	$-CH_3$	-H	-S-	-H	$-SCH_3$	-NH-	65.0	>250.0	>250.0
7e	SCA-106	$-CH_3$	$-CH_3$	-H	-S-	-Cl	$-SCH_3$	-NH-	30.0	50.0	50.0
7f	SCA-153	-F	-H	-H	-S-	-Cl	$-SCH_3$	-NH-	<50.0	200.0	175.0
7g	SCA-155	-F	-F	-H	-S-	-Cl	$-SCH_3$	-NH-	>100.0	50.0	41.6
7h	SCA-159	$-OCH_3$	$-OCH_3$	-H	-S-	-Cl	$-SCH_3$	-NH-	<50.0	100.0	>250.0
7i	SCA-161	-H	-H	$-CF_3$	-S-	-Cl	$-SCH_3$	-NH-	<50.0	25.0	14.6
7j	SCA-157	$-CF_3$	-H	-H	-S-	-Cl	$-SCH_3$	-NH-	<50.0	>250.0	>250.0
9a	SCA-111	$-CH_3$	$-CH_3$	-H	-S-	-Cl	-H	-NH-	>200.0	>250.0	>250.0
9b	SCA-110	$-CF_3$	$-CF_3$	-H	-S-	-Cl	-H	-NH-	100.0	35.4	18.8
12a	SCA-112	$-CF_3$	$-CF_3$	-H	-S-	-Cl	-SPh	-NH-	20.0	3.1	1.8
12b	SCA-113	$-CH_3$	$-CH_3$	-H	-S-	-Cl	-SPh	-NH-	50.0	>250	12.5
12c	SCA-114	$-CF_3$	$-CF_3$	-H	-S-	-Cl	-OPh	-NH-	9.0	8.3	3.1
12d	SCA-130	$-CF_3$	$-CF_3$	-H	-S-	-Cl	$-S(CH_2)_4CH_3$	-NH-	50.0	6.3	1.6
12e	SCA-138	$-CF_3$	$-CF_3$	-H	-S-	-Cl	$-S(CH_2)_4OH$	-NH-	25.0	43.8	25.0
12f	SCA-156	-F	-F	-H	-S-	-Cl	-SPh	-NH-	<50.0	31.3	20.8
12g	SCA-158	$-CF_3$	-H	-H	-S-	-Cl	-SPh	-NH-	<50.0	18.8	18.8
12h	SCA-160	$-OCH_3$	$-OCH_3$	-H	-S-	-Cl	-SPh	-NH-	<50.0	>250	≥100.0
12i	SCA-162	-H	-H	$-CF_3$	-S-	-Cl	-SPh	-NH-	<50.0	12.5	8.3
12j	SCA-163	$-OCH_3$	-H	-OH	-S-	-Cl	-SPh	-NH-	<50.0	>250	≥250.0
12k	SCA-154	-F	-H	-H	-S-	-Cl	-SPh	-NH-	<50	83.3	175.0
15	SCA-133	$-CF_3$	$-CF_3$	-H	-S-	-Cl	$-SCH_3$	-O-	200	>100	>250.0

[a] Compound concentration required to inhibit *Ec*SecAN68 ATPase activity by 50%. [b] Lowest compound concentration that inhibits bacterial growth after 24 h incubation at 37 °C; *E. coli* NR698 (with an outer membrane mutation resulting in increased drug permeability) and *S. aureus* 6538, representing Gram-negative and Gram-positive bacteria to screen all compounds.

Table 2. SAR tests for class IIA compounds.

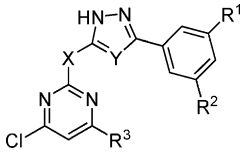

Compd	SCA	R^1	R^2	Y	X	R^3	IC_{50} [μM][a] *Ec*SecAN68	MIC [μM][b] *E. coli* NR698	MIC [μM][b] *S. aureus* 6538
16a	SCA-124	$-CF_3$	$-CF_3$	-NH-	-S-	-Cl	50.0	12.5	6.3
16b	SCA-116	$-CH_3$	$-CH_3$	-NH-	-S-	-Cl	>50.0	>164.0	100.0
16c	SCA-139	$-CF_3$	$-CF_3$	-NH-	-O-	-Cl	<50.0	250.0	37.5
16d	SCA-152	-H	-F	-NH-	-S-	-Cl	>100.0	200.0	≥100.0
16e	SCA-131	$-CF_3$	$-CF_3$	-NH-	-S-	$-NHCH_2Ph$	>50.0	≥250.0	50.0
17	SCA-135	$-CF_3$	$-CF_3$	-O-	-S-	-Cl	70.0	>250.0	18.8
18	SCA-140	$-CF_3$	$-CF_3$	-NH-	-O-	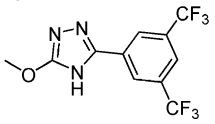	<50.0	>250.0	250.0

[a] Compound concentration required to inhibit *Ec*SecAN68 ATPase activity by 50%. [b] Lowest compound concentration that inhibits bacterial growth after 24 h incubation at 37 °C.

Table 3. SAR tests for class IIB and III compounds.

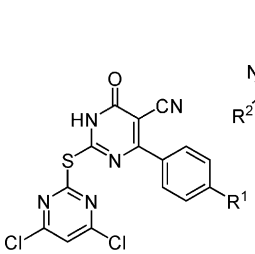

20a, **20b**

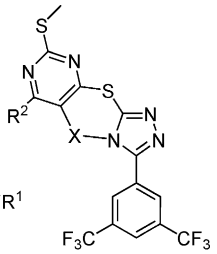

24, **25**, **26**

Compd	SCA	R^1	Y	R^2	IC_{50} [μM][a] *Ec*SecAN68	MIC [μM][b] *E. coli* NR698	*S. aureus* 6538
20a	SCA-127	-Br	N/A	N/A	< 50.0	> 250.0	> 250.0
20b	SCA-137	-Et	N/A	N/A	< 50.0	> 250.0	> 250.0
24	SCA-174	N/A	-CH=N-	-Cl	< 25.0	12.5	3.1
25	SCA-177	N/A	$-CH_2NH-$	-Cl	46.0	> 250.0	> 100.0
26	SCA-175	N/A	$-CH_2NH-$	-H	50.0	> 100.0	> 100.0

[a] Compound concentration required to inhibit *Ec*SecAN68 ATPase activity by 50%. [b] Lowest compound concentration that inhibits bacterial growth after 24 h incubation at 37 °C.

any other substituent (compounds **7f**–**7i**) significantly decreased the bacteriostatic effect, suggesting that the two trifluoromethyl groups are important for inhibition. Changing triazole to oxadiazole in the structure decreased inhibition greatly, suggesting that the triazole group is very important (compound **15**). Replacing the methylthio group with hydrogen decreased inhibitory capacity (compound **9b**), yet the methylthio group could be replaced with a phenylthio (**12a**) or phenoxy group (**12c**) without significantly changing the inhibitory effects.

Among all the compounds, **7b** (SCA-107) and **12a** (SCA-112) are the two most potent analogues developed from this study. We therefore focused on these two compounds, together with the original lead compound **1**, for further evaluation. As discussed in previous studies,[4c,15] monitoring the inhibitory activity toward the soluble form of *Ec*SecAN68 is a good initial screen. However, gauging inhibitory potency in the membrane lipid environment by using either an ion current channel activity assay or protein translocation assay seems to correlate more closely with antimicrobial activity.[8] We therefore subjected compounds **1**, **7b**, and **12a** to such assays, and found that the IC_{50} values for **7b** and **12a** were ~1.5–2.0 μM in the membrane protein translocation assay using *Ec*SecA and 2.0–4.8 μM in the SecA–liposomes translocation assay (Table 4). We also examined these SecA inhibitors using the channel activity assay in oocytes[8,18] (Table 5). These compounds showed very effective inhibition of the ion channel activity of *Ec*SecA, with IC_{50} values of ~1.3–2.4 μM. We also examined the effects of these compounds on the ion channel activity of SecA purified from other bacterial strains and then reconstituted with liposomes or cognate membranes. Table 5 shows that these compounds are also very effective against SecA from both Gram-positive and Gram-negative bacteria, with IC_{50} values ranging from 0.7 to 2.6 μM. The inhibitory potencies in the ion channel and protein translocation assays correlate very well with antimicrobial results (see Tables 1–4 and the section below), demonstrating once again what we reported earlier, that is: 1) the *Ec*SecAN68 assay is appropriate for the initial

Table 4. Inhibition of various SecA ATPase and in vitro protein translocation activities of *Ec*SecA.

Compd	IC_{50} [μM] ATPase activity *Ec*SecAN68	*Ec*SecA[a]	*Ec*SecATn[b]	Translocation activity Membrane[c]	SecA–liposomes[d]
1	18.0	32.0	20.0	7.0	ND
7b	30.0	> 200.0	28.0	1.5	2.0
12a	20.0	> 200.0	ND	2.0	4.8

[a] Intrinsic *Ec*SecA ATPase activity is that of full *Ec*SecA without membrane and proOmpA. [b] Translocation ATPase activity is that of *Ec*SecA in the presence of urea-washed *E. coli* BA13 membrane) and proOmpA. [c] In vitro translocation activity with membrane was determined by using OmpA-depleted and urea-washed 773 membranes and immunoblots to determine the translocation efficiency of proOmpA. [d] In vitro translocation activity with SecA–liposomes was determined by using reconstituted SecA-only liposomes and immunoblots to determine the translocation efficiency of proOmpA.

Table 5. Inhibition of ion channel activity of various SecA–liposomes in oocytes.

Compd	IC_{50} [μM][a] *Ec*SecA	*Sa*SecA1	*Ba*SecA1	*Bs*SecA	*Sp*SecA
1	2.4	1.6	1.5	2.6	1.0
7b	1.6	0.6	0.7	2.1	0.7
12a	1.3	1.0	1.0	2.3	1.3

[a] Ion channel activity of SecA-only liposomes was determined by adding reconstituted SecA–liposome complex into oocytes and recording the current induced by proOmpA; *Ec*SecA: *E. coli* SecA, *Sa*SecA1: *S. aureus* SecA1, *Ba*SecA1: *B. anthracis* SecA1, *Bs*SecA: *B. subtilis* SecA, *Sp*SecA: *Streptococcus pyogenes* SecA.

rapid screening, and 2) the protein translocation and ion channel activity assays provide numerical values of inhibitory activity that more closely parallel the antimicrobial efficacy. Corollary to these points is our examination of the effect of these three inhibitors on full-length SecA in solution (Table 4). As discussed previously,[15] the full-length Sec protein has an inhibitory/regulatory C terminus. In a non-membrane environment, the IC_{50} values of SecA inhibitors tend to be much higher than those obtained from the *Ec*SecAN68, channel activity, and protein translocation assays. Therefore, the IC_{50} values obtained from the full-length SecA assay in solution must be analyzed with the effect of the inhibitory/regulatory C terminus taken into consideration.

Thus far, the correlation between the inhibitory potency data from the channel activity and protein translocation assays and the antimicrobial data is consistent with the notion that the antimicrobial results (Tables 1–5) are largely due to SecA inhibition. To further examine this correlation, we conducted protein pull-down work. We synthesized a biotinylated analogue of **7b** (SCA-256), which was used to carry out the protein pull-down assay (Figure 3), the results of which showed

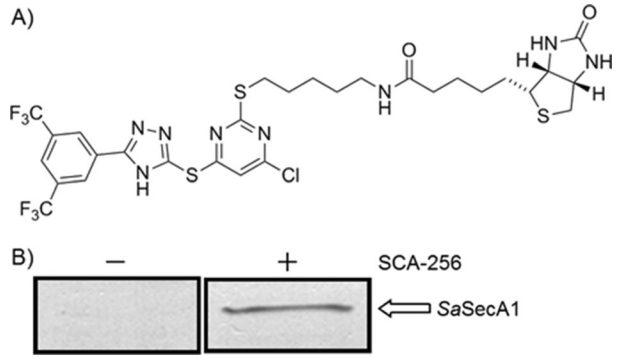

Figure 3. Validation of *Sa*SecA1 as a drug target by pull-down assay: a) Structure of SCA-256. b) Whole-cell lysate of *S. aureus* ATCC 6538 was mixed with SCA-256 (biotinylated **7b** analogue) for 1 h, then streptavidin magnetic beads were used to pull out proteins that interact with SCA-256. The interaction between *Sa*SecA1 and SCA-256 was examined by western blot with the cross-reacting *Ec*SecA antibody (1:5000 dilution). The synthesis of SCA-256 is described in the Supporting Information.

that SCA-256 maintains a reasonable level of inhibitory activity toward *Ec*SecAN68 ATPase ($IC_{50} \approx 60$ μM). The western blot results show that SCA-256 can recognize and pull down *Staphylococcus aureus* (*Sa*)SecA1 from whole-cell lysates (Figure 3B). Such results demonstrated the specific interactions between SecA and the inhibitors, further supporting the notion that *Sa*SecA1 is a target of this group of inhibitors. However, as with any protein pull-down work, rarely is only one protein pulled down. This is no exception for SCA-256. There are many factors that could contribute to such results and still be consistent with SecA being the key target for the antimicrobial effects of these inhibitors. Furthermore, it should be noted that the channel activity and protein translocation with SecA-only liposomes clearly showed the specific inhibition of SecA functional activity.

To better understand the mechanism of inhibition in view of the difference on SecA ATPase activity and functional activities with lipid/membranes, we conducted inhibition kinetics studies of SecA–liposome channel activity using **7b** (SCA-107) as a representative. Figure 4 shows that **7b** is a noncompetitive inhibi-

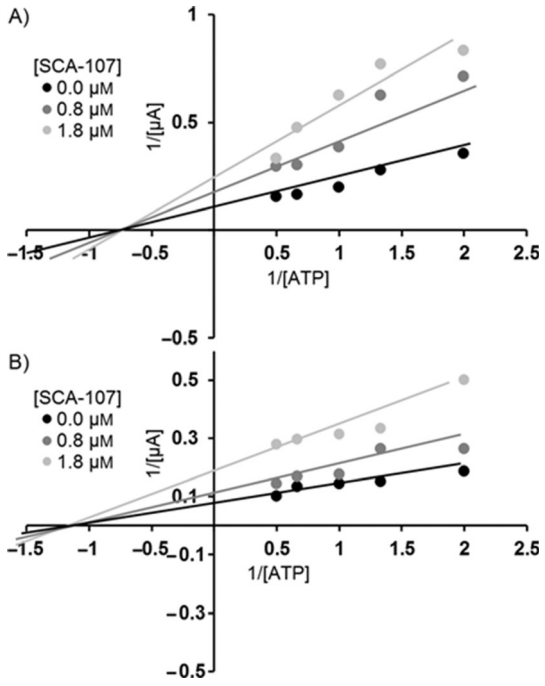

Figure 4. Ion channel activity against *Ec*SecA and *Sa*SecA1: The ion channel activity of SecA–liposomes was determined by adding reconstituted SecA–liposome complex into oocytes and recording the current induced by proOmpA. *Ec*SecA: *E. coli* SecA; *Sa*SecA1: *S. aureus* SecA1.

tor of *Ec*SecA and *Sa*SecA. Such results support the idea that the inhibitor does not bind directly in the ATP binding pocket. Molecular modeling suggests that **7b** partially blocks the entry of the ATP binding site (Figure 5). To gain an initial understanding of the possible binding site for these SecA inhibitors, docking studies were conducted with the SYBYL version 2.0 software package. Figure 5A shows that SCA-107 resides at the interface of monomers A and B, slightly toward the A monomer; Figure 5B shows the individual amino acid residues flanking SCA-107.

As discussed above, SecA is a conserved protein in bacteria. Thus there are good reasons to believe that SecA inhibitors can function as broad-spectrum antimicrobials. Our SecA inhibition data certainly support this notion. To examine this further, we evaluated the inhibitory effects of **1** (SCA-21), **7b** (SCA-107), and **12a** (SCA-112) against various strains of bacteria (Table 6). The results show that these three inhibitors have excellent antimicrobial effects, with MIC values between 0.8 and 25 μM, which are also similar to results for the inhibition of SecA-specific functions in the channel activity and protein translocation assays (Tables 4 and 5), and further support the idea that the antimicrobial target is SecA. In addition to bacteriostatic effects, hit compound **1** also exhibits bactericidal

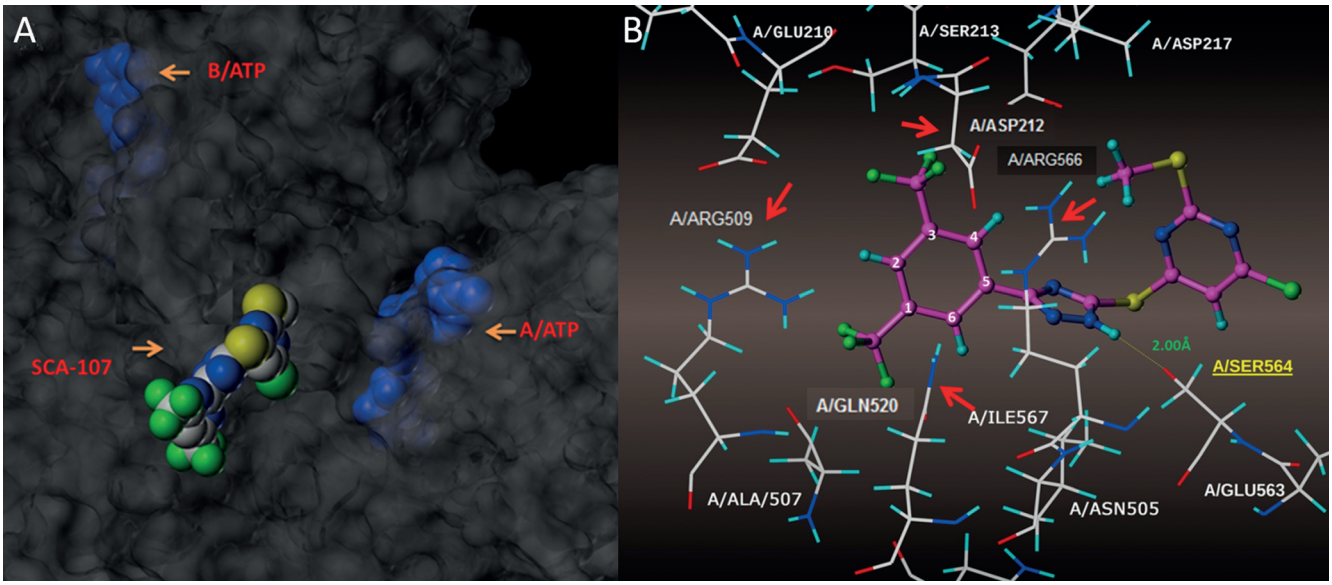

Figure 5. Molecular modeling of **7b** (SCA-107) binding in *Ec*SecA: A) Docking was performed with SYBYL 2.0 using PDB ID: 2FSG with SecA dimers A and B. Compound **7b** binds to the interface of the A and B monomers, closer to A (6 Å), partially blocking the entrance to the ATP site. B) SCA-107 (ball-and-stick structure) surrounded by residues of the *Ec*SecA active site. Red arrows indicate residues that are in SCA-107 vicinity but do not form bonds with the molecule.

Table 6. Bacteriostatic effects against various bacterial strains.[a]

Compd	MIC [μM][b]							
	E. coli NR698	*B. subtilis* 168	*B. anthracis* Sterne	*S. aureus* 6538	*S. aureus* Mu50	*S. aureus* N315	*S. aureus* Mu3	*S. aureus* Newman
1	25	6.3	6.3	12.5	ND	ND	ND	ND
7b	5.2	1.6	3.1	3.1	1.6	0.8	3.1	1.6
12a	3.1	0.8	1.6	1.8	0.8	0.8	1.6	ND

[a] Log-phase cells were diluted to $OD_{600} \approx 0.05$, followed by incubation with varying concentrations of compounds for 16 h at 37 °C. [b] Minimal compound concentration required to inhibit cell growth.

effects, with generally more than 2 log units decrease in CFU values at 25 μM against some *S. aureus* strains, as listed in Table 7. Compound **7b** decreased the CFU count of *S. aureus* Mu50 by 2 log units at 50 μM (Figure 6).

Some methicillin-resistant *S. aureus* (MRSA) strains acquire multidrug resistance in addition to their resistance to methicillin. We further examined the efficacy of our inhibitors against one strain, Mu50, in comparison with antibiotics in clinical use. The results show that **7b** (SCA-107, MIC: 0.75 μg mL^{-1}) and **12a** (SCA-112, MIC: 0.43 μg mL^{-1}) are more effective than most clinically used antibiotics including ampicillin (1000 μg mL^{-1}, >1300-fold), polymyxin B (31 μg mL^{-1}, >40-fold), erythromycin (1250 μg mL^{-1}, >1600-fold), tetracycline (63 μg mL^{-1}, >80-fold), kanamycin (1000 μg mL^{-1}, >1300-fold), rifampicin (1000 μg mL^{-1}, >1300-fold), norfloxacin (250 μg mL^{-1}, >330-fold), and even vancomycin (8 μg mL^{-1}, 10-fold for **7b**, 18-fold for **12a**), the latter of which is considered as the last-resort drug for treating many drug-resistant bacterial infections. These SecA inhibitors also exert bactericidal effects on a wide range of bacteria, including *S. aureus* Mu50, *S. aureus* N6538,

Table 7. Antimicrobial activities against *S. aureus* efflux strains.[a]

	Compd	SCA	WT 8325-4	NorA$^-$K1758	NorA^{++}K2361	MepA$^-$K2908	MepA^{++}K2068
Bacteriostatic MIC [μM]	**1**[b]	SCA-21	8	8	8	8	6
	7b	SCA-107	2.1	3.1	3.1	2.1	3.1
	12a	SCA-112	1.6	1.6	1.8	1.0	1.3
Bactericidal effect log [decrease CFU]	**1**	SCA-21	3	3	4	2	3

[a] Deletion (NorA$^-$, MepA$^-$) and overexpression (NorA^{++}, MepA^{++}) of NorA and MepA efflux pump strains, K1758, K2361, K2908, and K2068 are derivatives from *S. aureus* 8325-4. Bactericidal effects were determined by counting CFU after 1 h treatment at 37 °C with compounds at 25 μM concentration. [b] The initial MIC tested for compound **1** was from the tube assay.

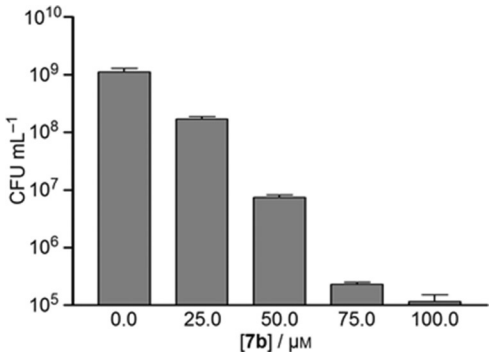

Figure 6. Bactericidal effect of **7b** (SCA-107) against *S. aureus* Mu50: Bactericidal effects were determined by counting CFU after 2 h treatment with various concentrations of **7b**.

and *B. anthraces* Sterne (Table 6, and data not shown). We previously described two other classes of structurally different SecA inhibitors,[16b,17] and this novel class is the most effective in terms of both bacteriostatic and bactericidal activity.

Compared with other known antimicrobial targets, one of the unique features of SecA is that it functions as a membrane protein. Therefore, inhibitors should be able to access SecA without the need for intracellular accumulation. One consequence of this ready accessibility of SecA is that efflux pumps are not expected to affect the potency of SecA inhibitors. To assess this, we examined various MRSA strains, which are known to possess multidrug-resistance efflux pumps and thus render many drugs ineffective. The results showed that growth inhibition by these SecA inhibitors is independent of the level of efflux pump expression in these strains (Table 7). Such results are consistent with the notion that SecA may be accessible by this class of inhibitors from the extracellular matrix. SecA inhibitors may therefore exert their effect without the need to enter the cell, and thus have the capacity to attenuate the effect of efflux pumps, a major mechanism behind multidrug resistance.

All the evidence from inhibition of SecA-dependent protein translocation, channel activity kinetic studies, and antimicrobial studies indicate that these SecA inhibitors exert their antimicrobial effect by the inhibition of SecA functions in the membranes, and possess the ability to bypass or minimize the effects of efflux pumps.

Conclusions

In summary, we have synthesized and evaluated a new class of triazole-pyrimidine analogues as novel SecA inhibitors. Compounds **7b** (SCA-107) and **12a** (SCA-112) showed the most potent activities, with IC_{50} and MIC values in the low- to submicromolar range. In addition, results from target identification assays are consistent with SecA being a target. The inhibition of SecA-dependent channel activity and protein translocation correlates well with antimicrobial activity, further suggesting that these compounds exert their antimicrobial effect through SecA inhibition. However, this does not exclude the possibility of off-target effects in the antimicrobial assay. A unique feature of SecA is the fact that it is a widely conserved membrane protein, responsible for the secretion of virulence factors, and directly accessible from the extracellular matrix without the need for certain intracellular concentrations. All these combined suggest that SecA inhibitors have the potential for being developed as broad-spectrum antimicrobials, can attenuate the pathogenicity of bacteria by directly inhibiting virulence factor production, and can overcome the effect of efflux pumps, which are responsible for multidrug resistance.

Experimental Section

Chemistry

All reagents were purchased from Acros or Aldrich and were used as received. ^{1}H and ^{13}C NMR spectra were collected on a Bruker 400 NMR spectrometer. Mass spectrometric analyses were performed by the Mass Spectrometry facilities at Georgia State University. Molecular modeling was conducted with SYBYL-X 2.0, and the standard procedures provided in the manual were used. Specifically, Surflex-dock was used to dock ligands into the SecA crystal structure (PDB ID: 2FSG) using automatic docking. All standard parameters provided in SYBYL-X 2.0 were used for energy minimization of the crystal structure of SecA. The AMBER7 FF99 force field, along with the default parameters described in the manual, were used, and a maximum of 20 docking poses were generated for each molecule.

2-(3,5-Bis(trifluoromethyl)benzoyl)hydrazinecarbothioamide (4a): To a mixture of 3,5-bis(trifluoromethyl)benzoyl chloride (1 g, 3.63 mmol) in 25 mL tetrahydrofuran was added hydrazine carbothioamide (0.73 g, 7.98 mmol) slowly at 0–5 °C. The temperature was increased to room temperature, and the reaction was stirred overnight. The reaction was then stopped with the addition of saturated sodium carbonate, and the mixture was extracted with EtOAc (3×50 mL). The combined organic layers were washed with water and brine, and dried over Na_2SO_4. The solid was filtered off, and the solvent was evaporated under reduced pressure to afford a crude product, which was used directly for the next step.

5-(3,5-Bis(trifluoromethyl)phenyl)-4*H*-1,2,4-triazole-3-thiol (5a): To the crude product **4a** was added 5% sodium hydroxide solution (50 mL), and the mixture was heated at reflux for 5 h. Then 2 N HCl was added to adjust the mixture to pH ~6–7. The white solid was filtered, washed with water 3–5 times, and then dried under vacuum at room temperature to give **5a** as a white powder (423 mg, 65% overall for two steps). ^{1}H NMR (DMSO): δ = 13.71 (s, 1H), 13.62 (s, 1H), 7.54 (s, 2H), 7.14 (s, 1H), 2.31 ppm (s, 6H); ^{13}C NMR (DMSO): δ = 168.1, 148.3, 131.8, 131.4, 128.3, 126.5, 124.7, 124.3, 122.0 ppm; ESI-MS: 314.3 $[M+H]^+$.

5-(3,5-Bis(trifluoromethyl)phenyl)-4*H*-1,2,4-triazol-3-amine (5b): Synthesis of **5b** followed the same procedure as for **5a** in 64% yield as a white powder. ^{1}H NMR (DMSO): δ = 8.38 (s, 2H), 8.06 (s, 1H), 6.33 (s, 2H); ^{13}C NMR (DMSO): δ = 158.6, 156.1, 135.0, 131.3, 131.0, 125.5, 125.0, 122.3, 121.9 ppm; ESI-MS: 297.0 $[M+H]^+$.

5-(3,5-Bis(trifluoromethyl)phenyl)-1*H*-1,2,4-triazol-3-ol (5c): Synthesis of **5c** followed the same procedure as for **5a** in 56% yield as a white powder. ^{1}H NMR (DMSO): δ = 8.41 (s, 2H), 8.36 (s, 1H), 2.50 ppm (s, 2H); ^{13}C NMR (DMSO): δ = 165.1, 134.6, 131.3, 131.1, 130.7, 129.9, 127.4, 126.7, 124.7, 121.9 ppm; ESI-MS: 298.0 $[M+H]^+$.

5-(3-Fluorophenyl)-1*H*-1,2,4-triazole-3-thiol (5d): Synthesis of **5d** followed the same procedure as for **5a** in 66% yield as a white powder. ^{1}H NMR (DMSO): δ = 13.92 (s, 1H), 13.77 (s, 1H), 7.35–7.76 ppm (m, 4H); ^{13}C NMR (DMSO): δ = 167.6, 163.9, 161.5, 149.5, 131.9, 128.0, 122.2, 118.0, 113.0 ppm; HRMS-ESI (+): calcd for $C_8H_7N_3SF$: 196.03, found: 196.03 $[M+H]^+$.

5-(3,5-Difluorophenyl)-1*H*-1,2,4-triazole-3-thiol (5e): Synthesis of **5e** followed the same procedure as for **5a** in 67% yield as a white powder. ^{1}H NMR (DMSO): δ = 8.34 (s, 2H), 8.32 ppm (s, 1H); ^{13}C NMR (DMSO): δ = 131.9, 131.6, 131.5, 127.6, 125.0, 124.6, 121.9 ppm.

5-(4-(Trifluoromethyl)phenyl)-1*H*-1,2,4-triazole-3-thiol (5h): Synthesis of **5h** followed the same procedure as for **5a** in 72% yield as a white powder. ^{1}H NMR (DMSO): δ = 7.54 (s, 2H), 7.14 (s, 1H), 2.31 ppm (s, 6H); ^{13}C NMR (DMSO): δ = 167.3, 150.8, 138.7, 132.4, 125.7, 123.8 ppm.

4-((5-(3,5-Bis(trifluoromethyl)phenyl)-4*H*-1,2,4-triazol-3-yl)thio)-6-methyl-2-(methylthio)pyrimidine (7a): To compound **5a** (70 mg, 0.34 mmol) in 10 mL acetone was added potassium carbonate (65.2 mg, 0.47 mmol) and 4,6-dichloro-2-(methylthio)pyrimidine (**6a**, 36.3 mg, 0.2 mmol). The reaction mixture was stirred at room temperature overnight. Then the reaction was stopped with the addition of 4 N HCl, and extracted with EtOAc (3×30 mL). The combined organic layers were washed with water and brine, dried over Na_2SO_4, and filtered. After purification by silica gel column chromatography (hexane/EtOAc 10:1), **7a** (79 mg, 64%) was obtained as a white solid. ^{1}H NMR (DMSO): δ = 8.60 (s, 2H), 8.29 (s, 1H), 7.96 (s, 1H), 6.95 (s, 1H); 2.32 ppm (s, 6H); ^{13}C NMR (DMSO): δ = 171.4, 167.7, 162.7, 131.9, 131.6, 126.7, 124.8, 123.7, 122.1, 113.1 ppm; MS-ESI (+): calcd for $C_{16}H_{11}F_6N_5S_2$: 452.41, found: 452.04 $[M+H]^+$.

4-((5-(3,5-Bis(trifluoromethyl)phenyl)-4*H*-1,2,4-triazol-3-yl)thio)-6-chloro-2-(methylthio)pyrimidine (7b): Synthesis of **7b** followed the same procedure as for **7a** in 67% yield as a light brown solid. ^{1}H NMR (DMSO): δ = 15.50 (br s, 1H), 8.57 (s, 2H), 8.25 (s, 1H), 7.28 (s, 1H), 2.34 ppm (s, 3H); ^{13}C NMR (DMSO): δ = 172.7, 160.1, 131.8, 131.5, 131.2, 126.8, 124.8, 122.1, 113.0, 14.0 ppm; HRMS-ESI (+): calcd for $C_{15}H_8N_5S_2F_6Cl$: 471.9874, found: 471.9856 $[M+H]^+$.

4-((5-(3,5-Bis(trifluoromethyl)phenyl)-4*H*-1,2,4-triazol-3-yl)thio)-2-(methylthio)pyrimidine (7c): Synthesis of **7c** followed the same procedure as for **7a** in 62% yield as a white solid. ^{1}H NMR ($CDCl_3$): δ = 13.34 (br s, 1H), 8.60 (s, 2H), 8.39 (d, J = 5.6 Hz, 1H), 7.93 (s, 1H), 7.01 (d, J = 5.6 Hz, 1H), 2.57 ppm (s, 3H); ^{13}C NMR ($CDCl_3$): δ = 173.4, 164.7, 160.1, 156.2, 132.4, 132.3, 132.0, 126.5, 124.5, 123.1, 121.8, 114.0, 14.2 ppm; ESI-MS: 438.0 $[M+H]^+$; HRMS-ESI (+): calcd for $C_{15}H_{10}F_6N_5S_2$: 438.0282, found: 438.0280 $[M+H]^+$.

4-((5-(3,5-Dimethylphenyl)-4*H*-1,2,4-triazol-3-yl)thio)-2-(methylthio)pyrimidine (7d): Synthesis of **7d** followed the same procedure as for **7a** in 57% yield as a white solid. ^{1}H NMR (DMSO): δ = 8.78 (d, J = 5.2 Hz, 1H), 8.60 (d, J = 5.2 Hz, 1H), 7.92 (d, J = 5.2 Hz, 1H), 7.62 (m, 2H), 7.11 (s, 1H), 2.61 (s, 3H), 2.34 ppm (s, 6H); ^{13}C NMR (DMSO): δ = 166.1, 160.5, 157.9, 138.4, 132.4, 124.4, 116.9, 21.3, 14.2, 13.9 ppm; ESI-MS (+): 330.1 $[M+H]^+$; HRMS-ESI (+): calcd for $C_{15}H_{16}N_5S_2$: 330.0847, found: 330.0841 $[M+H]^+$.

4-Chloro-6-((5-(3,5-dimethylphenyl)-4*H*-1,2,4-triazol-3-yl)thio)-2-(methylthio)pyrimidine (7e): Synthesis of **7e** followed the same procedure as for **7a** in 76% yield as a white solid. ^{1}H NMR (DMSO): δ = 15.06 (br s, 1H), 7.64 (s, 2H), 7.15 (s, 2H), 2.37 (s, 3H), 2.34 ppm (s, 6H); ^{13}C NMR (DMSO): δ = 172.6, 160.0, 138.8, 132.5, 124.4, 112.7, 60.2, 21.3, 14.1 ppm; HRMS-ESI (+): calcd for $C_{15}H_{14}N_5S_2Cl$: 364.0457, found: 364.0457 $[M+H]^+$.

4-Chloro-6-((5-(3-fluorophenyl)-4*H*-1,2,4-triazol-3-yl)thio)-2-(methylthio)pyrimidine (7f): Synthesis of **7f** followed the same procedure as for **7a** in 46% yield as a white off solid. ^{1}H NMR (DMSO): δ = 7.87–7.85 (d, J = 7.6 Hz, 1H), 7.78–7.76 (d, J = 9.2 Hz, 1H), 7.62–7.56 (dd, J = 7.6, 5.6 Hz, 1H), 7.37–7.33 (t, J = 7.6 Hz, 1H), 7.23 (s, 1H), 2.50 (s, 3H), 2.34 ppm (s, 3H); ^{13}C NMR (DMSO): δ = 172.6, 170.8, 164.0, 161.5, 160.0, 131.9, 131.8, 122.7, 117.8, 117.6, 113.4, 113.1, 112.8, 14.04 ppm; ESI-MS (+): 354.0 $[M+H]^+$.

4-Chloro-6-((5-(3,5-difluorophenyl)-4*H*-1,2,4-triazol-3-yl)thio)-2-(methylthio)pyrimidine (7g): Synthesis of **7g** followed the same procedure as for **7a** in 47% yield as a white solid. ^{1}H NMR (DMSO): δ = 7.67–7.65 (m, 1H), 7.44 (m, 1H), 7.26 (s, 1H), 2.33 ppm (S, 3H).

4-Chloro-6-((5-(3,5-dimethoxyphenyl)-4*H*-1,2,4-triazol-3-yl)thio)-2-(methylthio)pyrimidine (7h): Synthesis of **7h** followed the same procedure as for **7a** in 59% yield as a brown solid. ^{1}H NMR (DMSO): δ = 15.01(s, 1H), 7.16 (s, 3H), 6.61 (s, 1H), 3.80 (s, 6H), 2.49 ppm (s, 3H); ^{13}C NMR (DMSO): δ = 172.5, 161.3, 160.0, 104.4, 102.9, 60.2, 55.8, 14.5 ppm; ESI-MS (+): 396.03 $[M+H]^+$.

4-Chloro-2-(methylthio)-6-((5-(4-(trifluoromethyl)phenyl)-4*H*-1,2,4-triazol-3-yl)thio)pyrimidine (7i): Synthesis of **7i** followed the same procedure as for **7a** in 52% yield as a white powder. ^{1}H NMR (DMSO): δ = 8.22–8.20 (d, J = 8.0 Hz, 2H), 7.90-7.88 (d, J = 8.0 Hz, 2H), 7.26 (s, 1H), 2.32 ppm (s, 3H); ^{13}C NMR (DMSO): δ = 172.6, 170.4, 160.0, 130.8, 130.5, 128.8, 126.5, 126.4, 123.3, 112.9, 14.9 ppm.

4-Chloro-2-(methylthio)-6-((5-(3-(trifluoromethyl)phenyl)-4*H*-1,2,4-triazol-3-yl)thio)pyrimidine (7j): Synthesis of **7j** followed the same procedure as for **7a** in 39% yield as a white solid. ^{1}H NMR (DMSO): δ = 8.46–7.85 (m, 5H), 2.51 ppm (s, 3H).

4-Chloro-6-((5-(3,5-dimethylphenyl)-4*H*-1,2,4-triazol-3-yl)thio)-pyrimidine (9a): Synthesis of **9a** followed the same procedure as for **7a** in 57% yield as a white solid. ^{1}H NMR (DMSO): δ = 15.07 (br s, 1H), 8.84 (s, 1H), 7.66 (s, 2H), 7.53 (s, 1H), 7.18 (s, 1H), 2.35 ppm (s, 6H); ^{13}C NMR (DMSO): δ = 160.4, 158.7, 138.86, 124.4, 118.0, 21.3 ppm; ESI-MS (+): 318.0 $[M+H]^+$.

4-((5-(3,5-Bis(trifluoromethyl)phenyl)-4*H*-1,2,4-triazol-3-yl)thio)-6-chloropyrimidine (9b): Synthesis of **9b** followed the same procedure as for **7a** in 47% yield as a white solid. ^{1}H NMR (DMSO): δ = 15.52 (br s, 1H), 8.85 (s, 1H), 8.61 (s, 2H), 8.31 (s, 1H), 7.66 ppm (s, 1H); ^{13}C NMR (DMSO): δ = 160.6, 158.8, 132.1, 131.8, 131.5, 131.1, 126.8, 124.8, 124.0, 122.1, 118.3 ppm; ESI-MS: 426.0 $[M+H]^+$.

4,6-Dichloro-2-(phenylthio)pyrimidine (11a): To a mixture of thiophenol (0.28 mL, 2.73 mmol), potassium carbonate (565 mg, 4.1 mmol) and 5 mL acetone in a 10 mL round-bottom flask was added **10** and 2,4,6-trichloropyrimidine (500 mg, 2.73 mmol) at room temperature. The mixture was kept stirring overnight. Then the solid was filtered off, and the reaction mixture was concentrated by evaporation under vacuum. The residue was purified by silica gel column chromatography (hexane/EtOAc 25:1) to give **11a** (600 mg), which was used directly in the next step without purification.

4-((5-(3,5-Bis(trifluoromethyl)phenyl)-4*H*-1,2,4-triazol-3-yl)thio)-6-chloro-2-(phenylthio)pyrimidine (12a): To a mixture of **5a** (470 mg, 1.5 mmol), potassium carbonate (276 mg, 2 mmol) and acetone (5 mL) in a 10 mL round-bottom flask, was added **11a** (300 mg) at room temperature. The reaction was kept stirring at

room temperature overnight. Then the solid portion was filtered off, and the residue after solvent evaporation was purified by silica gel column chromatography (hexane/EtOAc 25:1→10:1) to give **12a** as a white solid (478 mg, 51% for two steps). ^{1}H NMR (DMSO): δ = 15.34 (brs, 1H), 8.58 (s, 2H), 8.29 (s, 1H), 7.44 (m, 3H), 7.20 (m, 2H), 7.11 ppm (m, 1H); ^{13}C NMR (DMSO): δ = 171.9, 160.2, 135.1, 132.1, 131.8, 131.5, 129.7, 127.7, 126.8, 124.9, 124.0, 122.2, 114.1 ppm; ESI-MS (+): 534.0 $[M+H]^+$.

4-Chloro-6-((5-(3,5-dimethylphenyl)-4*H*-1,2,4-triazol-3-yl)thio)-2-(phenylthio)pyrimidine (12b): Synthesis of **12b** followed the same procedure as for **12a** in 56% yield as a white solid. ^{1}H NMR (CD_3OD): δ = 7.56 (m, 2H), 7.38 (m, 2H), 7.17 (m, 5H), 2.40 ppm (s, 6H); ^{13}C NMR (CD_3OD): δ = 172.6, 170.8, 160.0, 138.8, 138.6, 134.8, 132.1, 129.1, 128.7, 127.8, 126.5, 123.9, 123.8, 112.8, 20.1 ppm; ESI-MS (+): 426.1 $[M+H]^+$.

4-((5-(3,5-Bis(trifluoromethyl)phenyl)-4*H*-1,2,4-triazol-3-yl)thio)-6-chloro-2-phenoxypyrimidine (12c): Synthesis of **12c** followed the same procedure as for **12a** in 43% yield as a white solid. ^{1}H NMR (DMSO): δ = 15.52 (brs, 1H), 8.56 (m, 3H), 7.49 ppm (m, 7H); ^{13}C NMR (DMSO): δ = 170.5, 163.5, 161.8, 158.9, 152.2, 151.9, 131.8, 131.4, 130.5, 129.8, 126.9, 125.8, 124.8, 124.1, 122.1, 121.8, 112.7, 107.7, 103.1 ppm; ESI-MS (+): 518.0 $[M+H]^+$.

4-((5-(3,5-Bis(trifluoromethyl)phenyl)-4*H*-1,2,4-triazol-3-yl)thio)-6-chloro-2-(hexylthio)pyrimidine (12d): Synthesis of **12d** followed the same procedure as for **12a** in 36% yield as a white solid. ^{1}H NMR ($CDCl_3$): δ = 8.61 (s, 2H), 7.94 (s, 1H), 7.03 (s, 1H), 3.15–3.11 (t, J = 7.6, 7.2 Hz, 2H), 1.75–1.70 (m, 2H), 1.43–1.27 (m, 6H), 0.95–0.92 ppm (m, 3H); ^{13}C NMR ($CDCl_3$): δ = 173.9, 165.7, 160.5, 132.4, 132.1, 132.0, 126.4, 124.5, 123.1, 121.8, 117.8, 113.1, 31.5, 30.9, 30.8, 30.1, 28.3, 22.1, 13.8 ppm; ESI-MS: 528.1 $[M+H]^+$.

4-((4-((5-(3,5-Bis(trifluoromethyl)phenyl)-4*H*-1,2,4-triazol-3-yl)thio)-6-chloropyrimidin-2-yl)thio)butan-1-ol (12e): Synthesis of **12e** followed the same procedure as for **12a** in 33% yield as a white solid. ^{1}H NMR ($CDCl_3$): δ = 8.59 (s, 2H), 7.94 (s, 1H), 6.96 (s, 1H), 3.76–3.73 (m, 2H), 2.94–2.90 (m, 2H), 1.73–1.62 ppm (m, 4H); ^{13}C NMR ($CDCl_3$): δ = 173.3, 167.1, 160.4, 132.5, 132.2, 131.9, 127.1, 124.4, 123.3, 121.7, 113.0, 62.2, 31.1, 30.8, 25.5 ppm; HRMS-ESI (+): calcd for $C_{18}H_{14}ClF_6N_5OS_2$: 530.0316, found: 530.0318 $[M+H]^+$.

4-Chloro-6-((5-(3,5-difluorophenyl)-4*H*-1,2,4-triazol-3-yl)thio)-2-(phenylthio)pyrimidine (12f): Synthesis of **12f** followed the same procedure as for **12a** in 59% yield as a white solid. ^{1}H NMR ($CDCl_3$): δ = 7.56–7.43 (m, 7H), 6.50 ppm (s, 2H); ^{13}C NMR ($CDCl_3$): δ = 178.6, 164.5, 164.4, 162.3, 161.8, 158.3, 135.6, 131.0, 130.4, 126.0, 121.6, 108.6, 105.2 ppm.

4-Chloro-2-(phenylthio)-6-((5-(3-(trifluoromethyl)phenyl)-4*H*-1,2,4-triazol-3-yl)thio)pyrimidine (12g): Synthesis of **12g** followed the same procedure as for **12a** in 41% yield as a white solid. ^{1}H NMR ($CDCl_3$): δ = 8.15–8.13 (d, J = 7.6 Hz, 1H), 7.14–7.12 (d, J = 8.0 Hz, 1H), 7.72–7.59 (dd, J = 7.6, 8.0 Hz, 1H), 7.64–7.44 (dd, J = 8.8, 7.2 Hz, 2H), 7.21–7.14 (m, 3H), 6.34 ppm (s, 1H); ^{13}C NMR ($CDCl_3$): δ = 176.5, 159.2, 135.5, 131.5, 131.2, 130.6, 129.8, 128.8, 125.7, 123.6, 123.5, 122.4, 111.3 ppm.

4-Chloro-6-((5-(3,5-dimethoxyphenyl)-4*H*-1,2,4-triazol-3-yl)thio)-2-(phenylthio)pyrimidine (12h): Synthesis of **12h** followed the same procedure as for **12a** in 45% yield as a white solid. ^{1}H NMR ($CDCl_3$): δ = 7.56–7.55 (d, J = 4.4 Hz, 2H), 7.26 (m, 5H), 7.06 (s, 2H), 3.83 ppm (s, 6H); ^{13}C NMR ($CDCl_3$): δ = 176.1, 161.2, 159.2, 135.3, 130.6, 130.1, 126.3, 111.1, 104.4, 102.9, 55.6 ppm; HRMS-ESI (+): calcd for $C_{20}H_{16}ClN_5O2S_2$: 458.0526, found: 458.0567 $[M+H]^+$.

4-Chloro-2-(phenylthio)-6-((5-(4-(trifluoromethyl)phenyl)-4*H*-1,2,4-triazol-3-yl)thio)pyrimidine (12i): Synthesis of **12i** followed the same procedure as for **12a** in 59% yield as a white solid. ^{1}H NMR (DMSO): δ = 8.22–8.20 (d, J = 8.0 Hz, 2H), 7.90–7.88 (d, J = 8.0 Hz, 2H), 7.26 (s, H), 2.32 ppm (s, 3H); ^{13}C NMR (DMSO): δ = 172.6, 170.4, 160.0, 130.8, 130.5, 128.8, 128.4, 125.5, 123.0, 111.8, 14.0 ppm.

3-(5-((6-Chloro-2-(phenylthio)pyrimidin-4-yl)thio)-4*H*-1,2,4-triazol-3-yl)-5-methoxy phenol (12j): Synthesis of **12j** followed the same procedure as for **12a** in yield 31% yield as a white solid. ^{1}H NMR (DMSO): δ = 7.47–7.45 (d, J = 7.2 Hz, 2H), 7.21–7.19 (d, J = 7.2 Hz, 2H), 7.11–7.09 (d, J = 7.2 Hz, 1H), 6.95 (s, 2H), 6.54 (s, 1H), 6.07 (s, 1H), 3.81 ppm (s, 3H); ^{13}C NMR (DMSO): δ = 175.7, 160.3, 159.4, 158.6, 135.6, 131.9, 125.9, 110.8, 108.6, 104.1, 103.1, 58.8 ppm.

3-(5-((6-Chloro-2-(phenylthio)pyrimidin-4-yl)thio)-4*H*-1,2,4-triazol-3-yl)-5-fluorophenol (12k): Synthesis of **12k** followed the same procedure as for **12a** in 54% yield as a light brown solid. ^{1}H NMR ($CDCl_3$): δ = 7.68 (m, 1H), 7.62–7.60 (d, J = 9.2 Hz, 1H), 7.43–7.39 (dd, J = 9.2, 7.2 Hz, 3H), 7.23–7.13 (m, 4H), 6.32 ppm (s, 1H); ^{13}C NMR ($CDCl_3$): δ = 176.4, 169.3, 164.1, 159.2, 135.5, 130.7, 130.1, 126.1, 122.2, 122.1, 117.7, 117.4, 113.8, 113.6, 111.2 ppm; HRMS-ESI (+): calcd for $C_{18}H_{11}ClN_5S_2$: 416.0208, found: 416.0207 $[M+H]^+$.

5-(3,5-Bis(trifluoromethyl)phenyl)-1,3,4-oxadiazole-2-thiol (14): Synthesis of **14** followed the same procedure as for **5a** in 69% yield as a white solid. ^{1}H NMR ($CDCl_3$): δ = 11.7 (s, 1H), 8.44 (s, 2H), 8.09 ppm (s, 1H); ^{13}C NMR ($CDCl_3$): δ = 178.1, 158.8, 133.0, 126.4, 125.8, 124.4, 123.8, 121.1 ppm; HRMS-ESI (+): calcd for $C_{10}H_4F_6N_2OS$: 315.0021, found: 315.0027 $[M+H]^+$.

2-(3,5-Bis(trifluoromethyl)phenyl)-5-((6-chloro-2-(methylthio)pyrimidin-4-yl)thio)-1,3,4-oxadiazole (15): Synthesis of **15** followed the same procedure as for **7a** in 58% yield as a white solid. ^{1}H NMR ($CDCl_3$): δ = 8.57 (s, 2H), 8.12 (s, 1H), 7.21 (s, 1H), 2.35 ppm (s, 3H); ^{13}C NMR ($CDCl_3$): δ = 174.2, 165.5, 165.1, 161.0, 158.3, 133.4, 133.1, 127.0, 125.9, 123.9, 121.2, 113.0, 14.2 ppm; ESI-MS: 472.8 $[M+H]^+$; HRMS-ESI (+): calcd for $C_{15}H_8ClF_6N_4OS_2$: 472.9719, found: 472.9722 $[M+H]^+$.

2-((3-(3,5-Bis(trifluoromethyl)phenyl)-1*H*-1,2,4-triazol-5-yl)thio)-4,6-dichloropyrimi-dine(16a): Synthesis of **16a** followed the same procedure as for **7a** in 78% yield as a white solid. ^{1}H NMR ($CDCl_3$): δ = 8.59 (s, 2H), 7.95 (s, 1H), 7.37 ppm (s, 1H); ^{13}C NMR ($CDCl_3$): δ = 169.2, 162.1, 160.1, 132.5, 132.2, 131.8, 126.55, 124.4, 123.4, 121.7, 119.0, 116.7 ppm; ESI-MS: 461.9 $[M+H]^+$; HRMS-ESI (+): calcd for $C_{14}H_5Cl_2F_6N_5S$: 459.9637, found: 459.9638 $[M+H]^+$.

4,6-Dichloro-2-((3-(3,5-dimethylphenyl)-1*H*-1,2,4-triazol-5-yl)thio)pyrimidine (16b): Synthesis of **16b** followed the same procedure as for **7a** in 74% yield as a white solid. ^{1}H NMR (DMSO): δ = 15.1 (s, 1H), 7.64 (s, 2H), 7.52 (s, 1H), 7.17 (s, 1H), 2.35 ppm (s, 6H); ^{13}C NMR (DMSO): δ = 174.8, 161.4, 158.9, 157.5, 151.3, 136.8, 132.6, 128.0, 124.5, 118.3, 21.3 ppm; ESI-MS: 352.1 $[M+H]^+$; HRMS-ESI (+): calcd for $C_{14}H_{12}Cl_2N_5OS$: 352.0184, found: 352.0190 $[M+H]^+$.

4,6-Dichloro-2-((3-(3,5-dimethylphenyl)-1*H*-1,2,4-triazol-5-yl)oxy)pyrimidine (16c): Synthesis of **16c** followed the same procedure as for **7a** in 64% yield as a white solid. ^{1}H NMR ($CDCl_3$): δ = 8.56 (s, 2H), 8.11 (s, 1H), 7.66 ppm (s, 1H); ^{13}C NMR ($CDCl_3$): δ = 167.6, 165.6, 162.7, 160.4, 157.4, 133.4, 133.0, 127.1, 125.9, 124.9, 123.9, 121.2, 117.0 ppm; ESI-MS: 445.3 $[M+H]^+$.

4,6-Dichloro-2-((5-(3-fluorophenyl)-4*H*-1,2,4-triazol-3-yl)thio)pyrimidine (16d): Synthesis of **16d** followed the same procedure as for **7a** in 71% yield as a white solid. ^{1}H NMR ($CDCl_3$): δ = 7.77–7.75 (d, J = 7.2 Hz, 1H), 7.70–7.68 (d, J = 9.2 Hz, 1H), 7.45–7.39 (dd, J = 8.4, 7.2 Hz, 1H), 7.26 (s, 1H), 7.19–7.14 ppm (m, 1H); ^{13}C NMR ($CDCl_3$): δ = 171.8, 164.1, 161.7, 130.9, 129.0, 122.2, 118.1, 117.8, 116.3, 113.8, 113.6 ppm; HRMS-ESI (+): calcd for $C_{12}H_7Cl_2FN_5S$: 341.9784, found: 341.9783 $[M+H]^+$.

***N*-Benzyl-2-((3-(3,5-bis(trifluoromethyl)phenyl)-4*H*-1,2,4-triazol-5-yl)thio)-6-chloro-pyrimidin-4-amine (16e)**: Synthesis of **16e** followed the same procedure as for **7a** in 45% yield as a white solid. ^{1}H NMR ($CDCl_3$): δ = 7.55 (s, 3H), 7.42–7.27 (m, 6H), 6.75 (s, 1H), 2.39 ppm (s, 2H); ^{13}C NMR ($CDCl_3$): δ = 198.4, 143.5, 134.4, 130.5, 128.9, 128.2, 128.1, 127.6, 127.5, 127.1, 126.9, 126.6, 27.5 ppm.

2-(3,5-Bis(trifluoromethyl)phenyl)-5-((4,6-dichloropyrimidin-2-yl)thio)-1,3,4-oxadi-azole (17): Synthesis of **17** followed the same procedure as for **7a** in 62% yield as a white solid. ^{1}H NMR ($CDCl_3$): δ = 8.57 (s, 2H), 8.12 (s, 1H), 7.66 ppm (s, 1H); ^{13}C NMR ($CDCl_3$): δ = 167.6, 165.6, 162.7, 160.5, 157.4, 133.4, 127.2, 125.9, 124.9, 123.9, 121.2, 117.0 ppm; HRMS-ESI (+): calcd for $C_{14}H_5Cl_2F_6N_4OS$: 460.9445, found: 460.9465 $[M+H]^+$.

2-((3-(3,5-Bis(trifluoromethyl)phenyl)-1*H*-1,2,4-triazol-5-yl)oxy)-4-((5-(3,5-bis(trifluoro methyl)phenyl)-4*H*-1,2,4-triazol-3-yl)oxy)-6-chloropyrimidine (18): Synthesis of **18** followed the same procedure as for **7a** in 65% yield as a white solid. ^{1}H NMR ($CDCl_3$): δ = 8.53 (s, 4H), 8.12 ppm (s, 2H); ^{13}C NMR ($CDCl_3$): δ = 167.3, 165.5, 160.3, 157.8, 133.3, 133.0, 127.2, 125.9, 124.9, 123.9, 121.2, 14.1 ppm.

4-(4-Bromophenyl)-2-((4,6-dichloropyrimidin-2-yl)thio)-6-oxo-1,6-dihydropyrimidine-5-carbonitrile (20a): Synthesis of **20a** followed the same procedure as for **7a** in 45% yield as a white solid. ^{1}H NMR ($CDCl_3$): δ = 7.82–7.80 (d, J = 8.4 Hz, 2H), 7.66 (d, J = 8.4 Hz, 2H), 7.56 ppm (s, 1H); HRMS-ESI (+): calcd for $C_{15}H_7BrCl_2N_5OS$: 453.8855, found: 453.8932 $[M+H]^+$.

2-((4,6-Dichloropyrimidin-2-yl)thio)-4-(4-ethylphenyl)-6-oxo-1,6-dihydropyrimidine-5-carbonitrile (20b): Synthesis of **20b** followed the same procedure as for **7a** in 52% yield as a white solid. ^{1}H NMR ($CDCl_3$): δ = 7.93 (s, 1H), 7.72–7.70 (d, J = 7.6 Hz, 2H), 7.43–7.41 (d, J = 7.6 Hz, 2H), 7.38 (s, 1H), 2.80–2.74 (m, 2H), 1.31–1.24 ppm (m, 3H).

4-Amino-5-(3,5-bis(trifluoromethyl)phenyl)-4*H*-1,2,4-triazole-3-thiol (22): To a mixture of **21**, 3,5-bis(trifluoromethyl)benzhydrazide (2.7 g, 10 mmol) and carbon disulfide (1.14 g, 15 mmol) in 20 mL absolute ethanol was added KOH (0.84 g, 15 mmol) pellets, and the reaction was held at reflux for 6 h. The solvent was evaporated under vacuum to afford potassium dithiocarbazate as a white solid, which was treated with hydrazine monohydrate (1.6 mL, 25 mmol) in water and then heated at reflux for 4 h. The color of the reaction mixture changed to green with the evolution of hydrogen sulfide gas (lead acetate paper test and odor). Then the reaction mixture was cooled to room temperature, diluted with water (100 mL), and acidified with concentrated HCl. The resulting precipitate was filtered, washed thoroughly with cold water, and recrystallized from ethanol to give compound **22** as a white solid (2.62 g, 82%). ^{1}H NMR (DMSO): δ = 14.2 (s, 1H), 8.69 (s, 2H), 8.31 (d, J = 7.6 Hz, 1H), 5.86 ppm (s, 3H); HRMS-ESI calcd for $C_{10}H_7F_6N_4S$: 329.0290, found: 329.0294 $[M+H]^+$.

3-(3,5-Bis(trifluoromethyl)phenyl)-7-chloro-9-(methylthio)pyrimido[5,4-*f*][1,2,4]triazolo[3,4-*b*][1,3,4] thiadiazepine (24): A mixture of compound **22** (328 mg, 1 mmol) and compound **23**, 4,6-dichloro-2-(methylthio)pyrimidine-5-carbaldehyde (223 mg, 1 mmol) in DMF (6 mL) was heated at 60 °C for 4 h. After cooling to room temperature, 20 mL water was added. The precipitate was filtered off and the resulting solid was further purified by flash chromatography (hexane/EtOAc 1:1) to afford **24** as a white solid (380 mg, 76%). ^{1}H NMR (DMSO): δ = 8.88 (s, 1H), 8.50 (s, 2H), 8.38 (s, 1H), 2.63 ppm (s, 3H); HRMS (ESI) calcd for $C_{16}H_8ClF_6N_6S_2$: 496.9839, found: 496.9828 $[M+H]^+$.

3-(3,5-Bis(trifluoromethyl)phenyl)-7-chloro-9-(methylthio)-5,6-dihydropyrimido[5,4-*f*][1,2,4]triazolo[3,4-*b*][1,3,4] thiadiazepine (25): To a suspension of compound **24** (50 mg, 0.1 mmol) in absolute ethanol (2 mL) was added sodium borohydride (3.8 mg, 0.1 mmol) in one portion with stirring. The yellow solution formed was kept at room temperature for 2 h. The solvent was removed under reduced pressure, and the residue was washed with water and filtered. The resulting white solid was collected to give compound **25** (41 mg, 82%). ^{1}H NMR ($CDCl_3$): δ = 8.72 (s, 2H), 8.03 (s, 1H), 6.27 (t, J = 6.2 Hz, 1H), 4.52 (d, J = 6.2 Hz, 1H), 2.51 ppm (s, 3H); HRMS (ESI) calcd for $C_{16}H_{10}ClF_6N_6S_2$: 498.9996, found: 498.9991 $[M+H]^+$.

3-(3,5-Bis(trifluoromethyl)phenyl)-9-(methylthio)-5,6,7,8-tetrahydropyrimido[5,4-*f*][1,2,4]triazolo[3,4-*b*][1,3,4] thiadiazepine (26): To a suspension of compound **24** (50 mg, 0.1 mmol) in absolute ethanol (2 mL) sodium borohydride (38 mg, 1 mmol) was added in portions with stirring. The yellow solution formed was kept at room temperature for 2 h. The solvent was removed under reduced pressure, and the residue was washed with water and then filtered. The resulting white solid was collected to give compound **26** (20 mg, 40%). ^{1}H NMR ($CDCl_3$/CD_3OD 1:1): δ = 8.72 (s, 2H), 8.02 (s, 1H), 3.69 (d, J = 8.2 Hz, 4H), 2.51 ppm (s, 3H); HRMS (ESI) calcd for $C_{16}H_{13}F_6N_6S_2$: 467.0542, found: 467.0551 $[M+H]^+$.

Biology

Bacterial strains and culture conditions: *E. coli* NR698 (MC4100 *imp*4213),[19] an outer membrane leaky mutant strain, was kindly provided by Thomas J. Silhavy (Princeton University). *S. aureus* ATCC strains 6538 and 35556 were from the American Type Culture Collection. *S. aureus strains* Mu50, Mu3, and N315 were kindly provided by C.-D. Lu, and Newman strain from Z. Eichenbaum (Georgia State University). Five efflux-pump-related *S. aureus* strains 8325-4, K1758 (NorA$^-$), K2361 (NorA^{++}), K2908 (MepA$^-$), and K2068 (MepA^{++})[1d,20] were kindly provided by G. W. Kaatz (Wayne State University School of Medicine). *Bacillus subtilis* 168 and *Bacillus anthracis* Sterne were lab stocks. All strains were grown on Luria–Bertani (LB) broth or agar plates at 37 °C.

Chemicals: DMSO was purchased from Sigma. The initial 38 compounds for screening, including hit compound **1**, were purchased from Maybridge.

Protein purification: *Ec*SecA, *Sp*SecA, and *Bs*SecA were purified as described.[21] *Ec*SecAN68, a truncated mutant of *Ec*SecA containing the N-terminal catalytic domain, was purified as previously described.[16b,21b] The *SasecA1* gene was amplified from *S. aureus* ATCC35556 and cloned into pET-21d with a His_6 tag at the C terminus. The *BasecA1* gene was amplified from *B. anthra*cis Sterne, and cloned into pET-20b with a C-terminal His_6 tag. *Sa*SecA1 and *Ba*SecA1 were purified with a HisTrap affinity column and a Superdex-200 column (GE healthcare).

Liposome and membrane preparations: The preparation of liposomes was performed as described previously.[8] Briefly, *E. coli* total lipids (Avanti) were dried and resuspended in 150 mM KCl solution,

and sonicated in an ice-water bath until the solution became clear, usually 3–5 min, which resulted in an average liposome diameter of ~130 nm. The liposome solutions were aliquoted, and stored at −80 °C before use. The liposomes were frozen and thawed once for the experiments. The preparation of SecA-depleted native membranes from BA13 is as previously described.[18a,22] The BA13 cells were grown at 42 °C to deplete the SecA, and the cells were collected and lysed by French press as described. *E. coli* 773 is an *ompA*-deleted strain in lab stock; the membrane vesicles were prepared from sucrose gradients as described.[23]

ATPase assays for EcSecAN68 and EcSecA: ATPase activities were determined by malachite green colorimetric assay as described previously.[15,16b] Translocation ATPase was assayed in the presence of SecA-depleted membranes and proOmpA precursors. IC_{50} is the concentration of the compound that inhibits 50% of ATPase activities.

In vitro translocation activity of EcSecA: In vitro translocation activity of *Ec*SecA was determined by using OmpA-depleted 773 membranes and SecA–liposome as described previously.[8] Briefly, reconstituted liposomes, SecA, and proOmpA were added into the translocation buffer[8] separately before reaction. Liposomes at 12 μg or 4.5 μg of OmpA-depleted 773 membranes with various amounts of SecA were used in the 0.1 mL reaction mixtures. The reactions were carried out at 37 °C for 45 min, and the translocation mixtures were processed by immunoblots as previously described.[8] IC_{50} is the concentration of the compound that inhibits 50% of in vitro translocation activity.

Ion channel activity of SecA–liposomes in oocytes: Liposomes were prepared as described previously.[8,9,15,16b,24] Oocytes were obtained from live frog *Xenopus laevis* (Xenopus Express, Inc.) and injected with sample mixtures as described previously.[8,18b] Briefly, 50 nL sample mixtures containing 120 ng liposomes, 120 ng SecA, 14 ng proOmpA, 2 mM ATP, 1 mM $Mg(OAC)_2$, and various concentrations of inhibitors were injected into oocytes (average volume: 500 nL) using a Nanoject II injector. The voltage clamp adapted from an electrophysiological method was used to measure the opening of protein conducting channels as described previously.[8,18b] After injection, the oocytes were incubated at 23 °C for 3 h, then the ion current was recorded continuously for 1 min. The inward and outward currents were recorded to measure the net currents for channel opening. IC_{50} is the concentration of the compound that inhibits 50% ion channel activities of *Sa*SecA1.

Bacteriostatic effect: Bacteriostatic effects were tested according to the guidelines of the Clinical and Laboratory Standards Institute.[25] This assay was performed in a 96-well microtiter plate in triplicate in three separate experiments, as described previously, at 37 °C with shaking at 250 rpm for 24 h. MIC is the lowest concentration of inhibitor at which cells were unable to grow.

Bactericidal effect: Bactericidal effect was determined as described previously.[16b] Cells in log-phase growth ($OD_{600} \approx 0.5$) were mixed with various concentrations of inhibitors, and then incubated in an Eppendorf Thermomixer R (Brinkmann Instruments) at 37 °C with shaking (1000 rpm) for 1 or 2 h. Cultures were serially diluted with LB, spread on LB plates, and incubated at 37 °C overnight for determination of colony forming units (CFU). Bactericidal effect was determined by the decrease in CFU as described previously.

Pull-down assay: *S. aureus* ATCC 6538 was grown in LB medium at 37 °C overnight. Cells were then harvested by centrifugation (10000 *g*, 10 min, 4 °C), washed with TBST buffer (0.1 M Tris·HCl pH 7.0, 0.15 M NaCl, 0.1% Tween-20) and resuspended with TBST buffer containing EDTA-free cocktail protease inhibitors. The cells were broken by French press at 69 MPa. Unbroken cells were removed by centrifugation at 5000 rpm (3000 *g*). Whole-cell lysates were treated with PureProteome Streptavidin Magnetic Beads (Millipore) at 4 °C for 1 h to remove nonspecific binding. The supernatant was mixed beads with or without 400 μM SCA-256 at 4 °C for 1 h. The beads were washed with TBST buffer three times and were mixed with SDS sample buffer, and boiled for 15 min. Cross-reacting *Ec*SecA antibody (lab stock) was used to detect *Sa*SecA1 by western blot.

Acknowledgments

Financial support by the US National Institutes of Health (AI104168) and Fellowships from the Molecular Basis of Diseases Program at Georgia State University (J.S., A.S.C., Y.H.H., and W.C.) is gratefully acknowledged.

Keywords: antimicrobials · protein secretion · pyrimidines · SecA inhibitors · triazoles

[1] a) H. W. Boucher, G. H. Talbot, J. S. Bradley, J. E. Edwards, D. Gilbert, L. B. Rice, M. Scheld, B. Spellberg, J. Bartlett, *Clin. Infect. Dis.* **2009**, *48*, 1–12; b) Centers for Disease Control and Prevention (CDC), **2013;** www.cdc.gov/drugresistance/; c) L. Fernández, W. J. Gooderham, M. Bains, J. B. McPhee, I. Wiegand, R. E. W. Hancock, *Antimicrob. Agents Chemother.* **2010**, *54*, 3372–3382; d) G. W. Kaatz, F. McAleese, S. M. Seo, *Antimicrob. Agents Chemother.* **2005**, *49*, 1857–1864; e) I. Chopra, C. Schofield, M. Everett, A. O'Neill, K. Miller, M. Wilcox, J. M. Frère, M. Dawson, L. Czaplewski, U. Urleb, C. Courvalin, *Lancet Infect. Dis.* **2008**, *8*, 133–139.

[2] a) V. Briken, *Curr. Drug Targets* **2008**, *9*, 150–157; b) H. Cao, R. L. Baldini, L. G. Rahme, *Annu. Rev. Phytopathol.* **2001**, *39*, 259–284.

[3] a) V. A. M. Gold, S. Whitehouse, A. Robson, I. Collinson, *Biochem. J.* **2013**, *449*, 695–705; b) E. Or, D. Boyd, S. Gon, J. Beckwith, T. Rapoport, *J. Biol. Chem.* **2005**, *280*, 9097–9105; c) A. Economou, *Expert Opin. Ther. Targets* **2001**, *5*, 141–153; d) A. Abe, *Kansenshogaku Zasshi* **2009**, *83*, 94–100; e) V. T. Lee, O. Schneewind, *Genes Dev.* **2001**, *15*, 1725–1752; f) J. R. Scott, T. C. Barnett, *Annu. Rev. Microbiol.* **2006**, *60*, 397–423.

[4] a) K. Segers, H. Klaassen, A. Economou, P. Chaltin, J. Anné, *Anal. Biochem.* **2011**, *413*, 90–96; b) Y. H. Hsieh, Y. Huang, J. Jin, L. Yu, H. Yang, C. Jiang, B. Wang, P. C. Tai, *Biochem. Biophys. Res. Commun.* **2014**, *454*, 308–312; c) J. Jin, J. Cui, A. S. Chaudhary, Y. Hsieh, K. Damera, H. Zhang, H. Yang, B. Wang, P. C. Tai, *Bioorg. Med. Chem.* **2015**, *23*, 7061–7068; d) A. S. Chaudhary, W. Chen, J. Jin, P. C. Tai, B. Wang, *Future Med. Chem.* **2015**, *7*, 989–1007; e) Y. J. Huang, H. Wang, F. B. Gao, M. Li, H. Yang, B. Wang, P. C. Tai, *ChemMedChem* **2012**, *7*, 571–577.

[5] a) M. G. Schmidt, E. E. Rollo, J. Grodberg, D. B. Oliver, *J. Bacteriol.* **1988**, *170*, 3404–3414; b) A. P. Magiorakosa, A. Srinivasanb, R. B. Careyb, Y. Carmelic, M. E. Falagasd, C. G. Giskef, S. Harbarthg, J. F. Hindlerh, G. Kahlmeteri, B. Olsson-Liljequistj, D. L. Patersonk, L. B. Ricel, J. Stellingm, M. J. Struelensa, A. Vatopoulosn, J. T. Weberb, D. L. Monneta, *Clin. Microbiol. Infect.* **2012**, *18*, 268–281; c) I. R. Siboo, D. O. Chaffin, C. E. Rubens, P. M. Sullam, *J. Bacteriol.* **2008**, *190*, 6188–6196; d) N. W. Rigel, M. Braunstein, *Mol. Microbiol.* **2008**, *69*, 291–302.

[6] a) T. Chitlaru, O. Gat, Y. Gozlan, N. Ariel, A. Shafferman, *J. Bacteriol.* **2006**, *188*, 3551–3571; b) M. J. Sibbald, A. K. Ziebandt, S. Engelmann, M. Hecker, A. de Jong, H. J. Harmsen, G. C. Raangs, I. Stokroos, J. P. Arends, J. Y. Dubois, J. M. van Dijl, *Microbiol. Mol. Biol. Rev.* **2006**, *70*, 755–788; c) A. Walz, C. V. Mujer, J. P. Connolly, T. Alefantis, R. Chafin, C. Dake, J. Whittington, S. P. Kumar, A. S. Khan, V. G. DelVecchio, *Proteome Sci.* **2007**, *5*, 11.

[7] a) D. B. Oliver, *Mol. Microbiol.* **1993**, *7*, 159–165; b) J. Eichler, K. Rinard, W. Wickner, *J. Biol. Chem.* **1998**, *273*, 21675–21681; c) A. J. Driessen, P. Fekkes, J. P. van der Wolk, *Curr. Opin. Microbiol.* **1998**, *1*, 216–222.

[8] Y. H. Hsieh, H. Zhang, B. R. Lin, N. Cui, B. Na, H. Yang, C. Jiang, S. F. Sui, P. C. Tai, *J. Biol. Chem.* **2011**, *286*, 44702 – 44709.
[9] T. A. Rapoport, B. Jungnickel, U. Kutay, *Annu. Rev. Biochem.* **1996**, *65*, 271 – 303.
[10] a) M. Li, Y. J. Huang, P. C. Tai, B. Wang, *Biochem. Biophys. Res. Commun.* **2008**, *368*, 839 – 845; b) W. Chen, Y. J. Huang, S. R. Gundala, H. Yang, M. Li, P. C. Tai, B. Wang, *Bioorg. Med. Chem.* **2010**, *18*, 1617 – 1625.
[11] a) N. R. Rivera, J. Balsells, K. B. Hansen, *Tetrahedron Lett.* **2006**, *47*, 4889 – 4891; b) T. Plech, M. Wujec, A. Siwek, U. Kosikowska, A. Malm, *Eur. J. Med. Chem.* **2011**, *46*, 241 – 248; c) A. Saha, R. Kumar, R. Kumar, C. Devakumar, *J. Heterocycl. Chem.* **2010**, *47*, 838 – 845.
[12] S. S. Patil, R. P. Jadhav, A. A. Patil, S. V. Patil, V. D. Bobade, *J. Chem. Pharm. Res.* **2010**, *2*, 38 – 51.
[13] L. Salerno, F. Guerrera, M. Modica, G. Romeo, V. Pittala, M. A. Siracusa, I. Mereghetti, A. Cagnotto, T. Mennini, *Med. Chem.* **2007**, *3*, 551 – 560.
[14] S. P. Pardeshi, S. V. Patil, R. Patil, V. D. Bobade, *J. Chem. Pharm. Res.* **2014**, *6*, 675 – 681.
[15] Y. J. Huang, H. Wang, F. B. Gao, M. Li, H. Yang, B. Wang, P. C. Tai, *ChemMedChem* **2012**, *7*, 571 – 577.
[16] a) A. S. Chaudhary, W. Chen, J. Jin, P. C. Tai, B. Wang, *Future Med. Chem.* **2015**, *7*, 989 – 1007; b) J. Cui, J. Jin, Y. H. Hsieh, H. Yang, B. Ke, K. Damera, P. C. Tai, B. Wang, *ChemMedChem* **2013**, *8*, 1384 – 1393.
[17] A. S. Chaudhary, J. Jin, W. Chen, P. C. Tai, B. Wang, *Bioorg. Med. Chem.* **2015**, *23*, 105 – 117.
[18] a) B. R. Lin, Y. H. Hsieh, C. Jiang, P. C. Tai, *J. Membr. Biol.* **2012**, *245*, 747 – 757; b) B. R. Lin, L. M. Gierasch, C. Jiang, P. C. Tai, *J. Membr. Biol.* **2006**, *214*, 103 – 113.
[19] N. Ruiz, B. Falcone, D. Kahne, T. J. Silhavy, *Cell* **2005**, *121*, 307 – 317.
[20] G. W. Kaatz, V. V. Moudgal, S. M. Seo, *J. Antimicrob. Chemother.* **2002**, *50*, 833 – 838.
[21] a) R. J. Cabelli, K. M. Dolan, L. P. Qian, D. B. Oliver, *J. Biol. Chem.* **1991**, *266*, 24420 – 24427; b) X. Chen, T. Brown, P. C. Tai, *J. Bacteriol.* **1998**, *180*, 527 – 537; c) X. Chen, H. Xu, P. C. Tai, *J. Biol. Chem.* **1996**, *271*, 29698 – 29706.
[22] R. S. Osborne, T. J. Silhavy, *EMBO J.* **1993**, *12*, 3391 – 3398.
[23] a) Y. B. Yang, J. Lian, P. C. Tai, *J. Bacteriol.* **1997**, *179*, 7386 – 7393; b) Y. B. Yang, N. Yu, P. C. Tai, *J. Biol. Chem.* **1997**, *272*, 13660 – 13665.
[24] H. W. Wang, Y. Chen, H. Yang, X. Chen, M. X. Duan, P. C. Tai, S. F. Sui, *Proc. Natl. Acad. Sci. USA* **2003**, *100*, 4221 – 4226.
[25] Performance Standards for Antimicrobial Susceptibility Testing; 21st Informational Supplement (M100-S21), Clinical and Laboratory Standards Institute (CLSI), Wayne, PA (USA), **2011**.

Received: September 29, 2015
Published online on November 26, 2015